Mechanical Properties Comparison of Four Models, Failure Theories Study and Estimation of Thermal Expansion Coefficients for Artificial E-glass Polyester Composite

Dr. Muhannad Z. Khelifa*, **Dr. Mustafa S. Abdullateef***, **Hayder M. Al-Shukri****

Received on: 1/12/2010
Accepted on: 3/3/2011

Abstract

In this paper, the mechanical properties of artificial E-glass reinforced polyester composite were evaluated; the elastic properties and the strength of the composite were measured experimentally by tensile tests and then compared with the predicted values by theoretical four micromechanical constitutive models. The strength of the composite lamina and laminates were also determined experimentally and compared with five widely used theoretical failure theories. The lamination theory was also used to determine the strength of laminates by applying Hill- Tsai failure criterion. The theoretical models showed that the composite stiffness increases with increasing the fibre volume fraction and the volume fraction which gave the best fit to the experimental results of elastic modulus (E_1) corresponds to volume fraction (V_f) equal 0.37. The stiffness of a unidirectional lamina depends on the fiber orientation relative to the off-axis load direction, and it drops sharply as the fiber alignment angle increases. In addition, the prediction of thermal expansion coefficients of composite is carried out in the present analysis, whereas the values of the coefficient that estimated to be based on the mechanical properties of the certain composite theoretically and experimentally.

Keywords: E-glass polyester, Composite mechanical properties, Expansion thermal coefficient, Failure criteria theories

مقارنةُ الخواص الميكانيكيةِ لأربعة نماذج، دراسة نظرياتِ فشلٍ وحساب معامل التمدد لمادة الليف الزجاجي المدعوم بالبولستر المصنعة

الخلاصة

يستعرض البحث حساب الخواص الميكانيكية لمادة مركبة مصنعة من الليف الزجاجي المدعوم بالبولستر ،حيث تم إيجاد قيم الخواص المرنة و المتانة مختبريا بواسطة فحوصات الشد وبعد ذلك قورنت بالقيم المتوقعة من أربعة نماذج micromechanical نظريا. متانة الطبقة الواحدة وكذلك عدد من الطبقات للمادة المركبة تم حسابها مختبر يا وتمت المقارنة بخمس نظريات معيار للفشل نظريا.نظرية التصفيح lamination theory استخدمت لحساب قوة الطبقات بتطبيق معيار الفشل Hill- Tsai. بينت النتَائج نظريا إن زيادة المرونة للمادة المركبة مرتبطة بزيادة volume fraction (V_f) وان الأخير يعطي أفضل تقارب مع النتائج المختبرية لمعامل المرونة (E_1) عندما تكون(V_f) تساوي0.37 . متانة الطبقة من نوع unidirectional تعتمد على توجيهِ الليفَ نسبة إلى اتجاه حملِ خارجِ المحورَ، وكذلك تتناقص بشدّة بينما زاوية اصطفاف الليف تزداد. بالأضافة الى ذلك فان تخمينَ قيم معامل التمدد الحراري في المواد المركبة (مصنعة من الليف الزجاجي المدعوم بالبولستر) قد تم التطرق اليها في هذا البحث أيضاً. حيث تم حساب قيم المعاملات الحرارية الطولية والعرضية إعتماداً على قيم الخصائص الميكانيكية التي تم الحصول عليها للمادة المعنية بالبحث عملياً ونظرياً.

***Electromechanical Engineering Department, University of Technology/ Baghdad**
****General Directorate for Vocational Education, Ministry of Education/Baghdad**

Notations

$A_{c,f,m}$	Cross section area of composite, fiber and matrix, respectively.	m^2
C	Contiguity factor.	
$e_{m,f}$	Matrix & fiber ply thickness	mm
E	Young's modulus.	N/m^2
$E_{f,m}$	Young's modulus of the fiber, and matrix respectively.	N/m^2
$G_{i,j}$	Shear modulus in local and global coordinate	N/m^2
$K_{f,m}$	Bulk modulus of the fiber, and matrix respectively.	N/m^2
K*	Bulk modulus	
L , ΔL	Length, elongation of length respectively.	m
$M_{f,m}$	Weight fraction of fiber, and matrix, respectively.	
V_f, V_m	Volume fraction of fiber , and matrix respectively.	
X_t, (X_c)	Longitudinal and compressive tensile strength.	N/m^2
Y_t, (Y_c)	Transverse and compressive tensile strength.	N/m^2
α	Coefficient of thermal expansion.	
ε	Strain tensor.	
$\sigma_{f,m}$	Stress on fiber , and matrix respectively.	N/m^2
$\sigma_{i,j}$	Stress in the local and global coordinate directions.	N/m^2
$\nu_{i,j}$	Poisson's ratio in the local and global coordinate directions.	-
$\gamma_{i,j}$	Shear strain in the local and global coordinate directions.	-
$\tau_{i,j}$	Shear stress in the local and global coordinate directions.	N/m^2
σ_{ult}	UTS, ultimate tensile stress.	N/m^2
ξ	Transverse reinforcing factor.	-
θ	The orientation angle ply with respect to x-axis.	degree
σ_m	Mean stress.	N/m^2
σ_a	Stress amplitude.	N/m^2
σ_x	Failure stress at any angle (θ).	N/m^2
$\underline{\Sigma}$	Stress tensor	
I	Unit tensor	
ΔT	Change in temperature with respect to a reference temperature at which the stresses and strains are nil.	C^o

Introduction

The main properties that describe a composite material are the engineering constants and the strength properties of a single unidirectional lamina that make the laminated structure. The experimental evaluation of these properties is quite costly and time consuming because they are functions of several variables such as the individual constituents of the composite, fiber volume fraction, packing geometry and fabrication processes,[1]. Hence, analytical models to predict these properties were developed by researchers to aid the design of composites. Obrien, etal (2001) [2], investigated the influence of specimen preparation of glass polymer composites on the transverse tensile strength. They reported that polishing specimen edges had little, or no, effect on the transverse tension strength of 90^o laminate tested in bending tests. However, polishing the tension side of the specimens results lower strengths. Furthermore, specimens with polished edges and surfaces have larger variation in

results than the unpolished specimens.

Urban (2003) [3], he studied the crushing behavior of glass polyester composites in ship construction by carried out tensile and compression measurements on both unidirectional lamina and [±*45*] laminates under axial and off-axis loading. The progressive failure of the composite was also demonstrated from experimental measurements as well as in models based on lamination theory. El-Hajjar (2004) [4] presented analytical and experimental study on fracture behaviors of thick section glass-polyester composites including material characterization and constitutive modeling. In his study, he also performed tension and compression tests on off-axis unidirectional test specimens to extract stiffness. Micromechanical materials models were coupled with finite element analysis to predict the crack growth for various crack geometries. Parhi, et al (2001) [5] worked on the failure analysis of multiple delamination in composite laminate subjected to transverse static load as well as on impact. Finite element analysis based on simple multiple delamination model and Tsai Wu failure criteria [6] was used in his analysis. His findings are that delamination influences the first ply failure significantly and first ply failure always occurs at the last layer where bending curvature is highest. In addition, the first ply failure load and the critical impact or velocity was found to be relatively higher for cross-ply laminate compared to angle-ply laminate. Paris (2001) [7], presented the development of failure criteria theories which have concentrated on taking into account different local failure mechanisms such as fiber-matrix shearing and delamination, out of lamina failures, or specialized cases such as non-linearity in shear stress, nonlinearity in deformation under impact loads. Andrej Cherkaev (2004) [8], presented suggests a method for bounds for a anisotropic effective compliance S and anisotropic extension tensor α of a composite. One meets these problems dealing with composites made of materials that experience phase transition or thermal expansion. The bounds are independent of the structure of a composite and depend only on the moduli of the phases and their volume fractions. O. Sigmun et al (1996) [9], We design three-phase composites having maximum thermal expansion, zero thermal expansion, or negative thermal expansion using a numerical topology optimization method. It is shown that composites with effective negative thermal expansion can be obtained by mixing two phases of positive thermal expansions with a void phase.

In this paper the four models are used in the analysis of the experimental results of the glass polyester composite studied in the present investigation for estimated the mechanical properties. The strength of the composite lamina and laminates were also determined experimentally and compared with five widely used theoretical failure theories and the lamination theory was also used to determine the strength of laminates by applying Hill- Tsai failure criterion. Finally, the values of the expansion coefficient that estimated to be based on the mechanical properties.

Experimental Procedure:

(i) Materials:

E-glass fibers having density of 2.5 g/cm^3 and modulus of 72 GPa were used as the reinforcing material in polyester matrix. The polyester, Syropole 8340 IS, is unsaturated

resin with catalyst addition; having a density of 1.22 g/cm^3 and modulus of 2.82 GPa was used as the matrix material,[8].

(ii) Specimen Preparation:

Composite panels were prepared according to **ASTM** standard **D5687** and through a hand lay-up process. The panel thickness and lamina orientations were controlled by performing the lay-up process in a specially made mold frame [10], the 30x30 cm frame is made of steel plate in two sections, a 6 mm deep mold and 12 mm thick heavier cover, twelve vertical fastener bolts were welded to the base to assist holding the composite in situ after lay-up. The cover was applied to prevent any buckling occurring during the curing process; each layer thickness is controlled to be 1 mm by using a steel ruler fixed to the frame. The curing process was completed in 24 hrs at room temperature, followed by oven cure at 70^{o}C for three hours. The fiber volume fraction in the composite is 37% [11]. The specimens were cut out of the 30x30 cm panels and tested according to **ASTM D3039/D3030M** standards [12]. Four layer composite specimens were prepared at a layer thickness of 1mm. The cut edges were

polished in two stages in order to remove flaws and to obtain smooth and crack-free surfaces. Emery paper of grade 434 and 1000 were used for this purpose. The 4 mm thick specimen's dimensions are 250 mm by 25 mm and gage length of 150 mm. Unidirectional specimens were cut at 0°, 30°, 45°, 60°, and 90° angles with respect to the fiber direction. Angle-ply specimens with laminates at stacking arrangements of $[0/90]_s$, $[\pm 45]_s$, and $[-15/75]_s$, were also prepared. Figure (1) shows some specimens.

(iii) Tensile Tests Procedure

The graphical results obtained from the Instron's 1195 hydraulic machine Figure (2) tensile tests were translated into stress-strain graphs. A linear regression line was used to fit the linear portion of the graph where Hook's law applies. This portion of the stress-strain curve is that near the origin and before the yield point where the curve starts to deviate from linearity. The elastic modulus (E) is then calculated from the slope of the linear part of the curve where Hook's law applies: i.e.

$$E = \frac{F/A}{\Delta L/L}$$

The procedure was repeated for all the tensile test results of the composite specimens and the matrix specimen. The average values of the measurements are given in Table (1). The load was applied longitudinal at a constant rate of 1 mm/min until specimen failure occurred. The test results were continuously monitored on a chart recorder in the form of load in kg vs. the elongation of the specimen in mm at any instance during the course of each test. The maximum load-range possible by the machine is between 250 kg and 2500 kg. Tensile test specimens after failure are shown in Figure (3).

Theoretical Predictions of the Engineering Constants

Four theoretical models were used in order to compare the experimental results with calculated values using expressions given by these models.

(i)Longitudinal elastic modulus (E_1)

The longitudinal elastic modulus (E_1) for the unidirectional composite (0° cut) was calculated for the fiber volume

fraction in the range (V_f = *0 to 1*) by using equations of the various micromechanical models given below,[12].

A- Mechanics of Materials Model (SRoM)

$E_1 = E_f V_f + E_m V_m$ …..(2)

B-Halpin-Tsai Model

$E_1 = E_f V_f + E_m V_m$ …..(3)

C- Composite Cylinder assemblage Model (CCA)

$$E_1 = E_f V_f + E_m V_m - \frac{2E_m E_f (v_f - v_m)^2 V_m}{\{E_f [2v_m^2 V_f - v_m + v_f v_m - v_f - 1] + E_m [-1 - 2v_f v_f^2 + v_f - v_f v_f + 2v_f^2 + V_f]\}}$$

…..(4)

D-Tsai Elasticity Model with Contiguity Factor

$E_1 = C(E_f V_f + E_m V_m)$ $C \leq 1$.

…..(5)

(ii) Transverse elastic modulus (E_2)

The models also give expressions that calculate the transverse elastic modulus (E_2). These expressions vary to certain degree as their derivations are based on different hypothesis,[12].

A-Mechanics of Materials Model (SRoM)

$$\frac{1}{E_2} = \frac{V_f}{E_f} + \frac{V_m}{E_m} \quad \text{…..(6)}$$

B-Halpin-Tsai Model

$$E_2 = E_m . \frac{1 + \xi_1 \eta_1 V_f}{1 - \eta_1 V_f} \quad \text{…..(7)}$$

$$\eta_1 = \frac{E_f - E_m}{E_f + \xi_1 E_m}$$

ξ_1=2 gives accurate (E_2) values; transverse reinforcing factor

C- Composite Cylinder assemblage Model (CCA)

$E_2 = 2(1 + \nu_{23}) G_{23}$ …..(8)

where, $\nu_{23} = \frac{K^* - mG_{23}}{K^* + mG_{23}}$,

$$m = 1 + 4K^* \frac{\nu_{12}^2}{E_1}$$

The bulk modulus K^* of the composite under longitudinal plane strain is given by:

$$K^* = \frac{K_m (K_f + G_m) V_m + K_f (K_m + G_m) V_f}{(K_f + G_m) V_m + (K_m + G_m) V_m}$$

…..(9)

$$K_f = \frac{E_f}{2(1+\nu_m)(1-2\nu_f)},$$

$$K_m = \frac{E_m}{2(1+\nu_m)(1-2\nu_m)}$$

G_{23} is given by the positive solution of the quadratic equation:

D- Tsai Elasticity Model with Contiguity Factor (0 ≤ C ≤1).

$$K_f = \frac{E_f}{2(1-V_f)},\ G_f = \frac{E_f}{2(1+V_f)},\ K_m = \frac{E_m}{2(1-V_m)},\ G_m = \frac{E_m}{2(1+V_m)}$$

…..(10)

(iii) Poisson's Ratio (□12):

An expression to Poisson's ratio(□$_{12}$)as a function of volume fraction is also considered by the above four models,[13].

A-Mechanics of Materials Model (SRoM)

$\nu_{12} = \nu_f V_f + \nu_m V_m$ …..(11)

B-Halpin-Tsai Model

$\nu_{12} = \nu_f V_f + \nu_m V_m$ …..(12)

C- Composite Cylinder Assemblage Model (CCA)

$$\nu_{12} = \nu_f V_f + \nu_m V_m + \frac{V_f V_m (\nu_f - \nu_m)(2E_f \nu_m^2 + \nu_m E_f - E_f + E_m - E_m \nu_f - 2E_m \nu_f^2)}{(2\nu_m^2 V_f - \nu_m V_f - 1 - V_f) E_f + (2\nu_f^2 - V_f \nu_f^2 + V_f + \nu_f - 1) E_m}$$

…..(13)

D-Tsai Elasticity Model with Contiguity Factor.

A graphical presentation of the predicted values, using the above four models, is given in Figure (5).

$$\nu_{12}=(1-C)\frac{K_f V_f (2K_m+G_m)V_m + K_m V_m (2K_f+G_m)V_m}{K_f(2K_m+G_m)-G_m(K_f-K_m)V_m} + C\frac{K_m V_m (2K_f+G_f)+G_f(K_m-K_f)V_m}{(2K_m+G_f)+G_f(K_m-K_f)V_m}$$

(vi) In-Plane Shear Modulus (G_{12})

The expressions are given in terms of the shear modulus of the fiber (G_f) and the matrix (G_m),[13].

A-Mechanics of Materials Model (SRoM)

$$\frac{1}{G_{12}}=\frac{V_f}{G_f}+\frac{V_m}{G_m} \quad .....(14)$$

B- Halpin-Tsai Model

$$G_{12} = G_m \frac{1+\xi_2 \eta_2 V_f}{1-\eta_2 V_f} \quad .....(15)$$

$$\eta_2 = \frac{G_f - G_m}{G_f + \xi_2 G_m}$$

C- Composite Cylinder Assemblage Model (CCA)

$$G_{12} = \left(\frac{G_f(1+V_f)+G_m V_m}{G_f V_m + G_m(1+V_f)}\right) G_m \quad .....(16)$$

D-Tsai Elasticity Model with Contiguity Factor.

$$G_{12}=(1-C)G_m\frac{2G_f-(G_f-G_m)V_m}{2G_m+(G_f-G_m)V_m}+CG_f\frac{(G_f+G_m)-(G_f-G_m)V_m}{(G_f+G_m)+(G_f-G_m)V_m}$$

.....(17)

The experimental values of G_{12}, extracted from the angle ply tensile tests, are also included. In simplified mathematical notations, the apparent Young modulus E_x is expressed in terms of the angle of lamina (θ) and the engineering constants of the unidirectional lamina as:

$$\frac{1}{E_x}=\frac{1}{E_1}\cos^4(\theta)+\left(\frac{1}{G_{12}}-\frac{2\nu_{12}}{E_1}\right)\cos^2(\theta).\sin^2(\theta)+\frac{1}{E_2}\sin^4(\theta) \quad .....(18)$$

Unidirectional Laminate under off-axis Tensile Load

In order to compare the four models predictions of the apparent elastic modulus E_x (θ) at the full span of ($\theta = 0 - 90^o$) angle, the predicted values of the engineering constants from the four models were used in the calculations. In-plane shear strength of the lamina was extracted from the uniaxial tensile test of the [±45] laminate as **ASTM standards D3518-76** [11]. That is,

$$S_t = \frac{S_t(\pm 45)}{2} \quad .....(19)$$

The longitudinal ultimate strength X_t is determined from the strength of [0_4] laminate test. The transverse ultimate strength Y_t is determined from the strength of [90_4] laminate test. The results are:

X_t = 95.99 *MPa*

Y_t =16.93 *MPa*

S_t = 25.80 *MPa*

Failure Criteria Theories

The failure theories are based on the stresses in the material at local axes because a lamina is orthotropic and its properties are different at different angles. In the case of unidirectional lamina, there are two material axes of which one is parallel to the fibres and one is perpendicular to the fibres. Thus, there are four normal strength parameters. The five strength parameters of a unidirectional lamina are therefore,[14].

$(\sigma_1^t)_{ult} = X_t$ = ultimate longitudinal tensile strength (direction *1*)

$(\sigma_1^t)_{ult} = X_c$ = ultimate longitudinal compressive strength (direction *1*)

$(\sigma_2^t)_{ult} = Y_t$ = ultimate transverse tensile strength (direction *2*)

$(\sigma_2^c)_{ult} = Y_c$ = ultimate transverse compressive strength (direction *2*)

$(\tau_{12})_{ult} = S_t$ = ultimate in-plane shear strength (in-plane *1-2*)

(i). Maximum Stress Failure Criterion

The limit criterion predicts ply (lamina) failure based on the individual stress or strain components in the ply. In mathematical terms, the lamina is considered to be failed if any of the following conditions is violated, [15].

$\sigma_1/X_t \geq 1; \quad -\sigma_1/X_c \geq 1$

Tensile and compressive fibre failure

$\sigma_2/X_t \geq 1; \; -\sigma_2/X_t \geq 1$

Tensile and compressive matrix failure

$\tau_{12}/S_t \geq 1$

Shear failure

The failure criterion can be expressed in a simplified form by the following equation where the strength of the lamina σ_x is determined for laminas at any angle (θ).

$$\sigma_x = \min\left[\frac{\sigma_1\cos^2(\theta)}{X_t}, or, \frac{\sigma_2\sin^2(\theta)}{Y_t}, or, \frac{\tau_{12}\cos(\theta).\sin(\theta)}{S_t}\right]$$

..... (20)

(ii) Tsai-Hill Failure Criterion:

For an applied stress σ_x, in global coordinates the failure criterion takes the following form:

$$\left(\frac{\cos^2(\theta)}{X_t}\right)^2 + \left[\frac{\cos(\theta)\sin(\theta)}{X_t}\right]^2 + \left(\frac{\sin^2(\theta)}{Y_t}\right)^2 + \left(\frac{\cos(\theta)\sin(\theta)}{S_t}\right)^2 < \left(\frac{1}{\sigma_x^2}\right)$$

.... (21)

(iii) Tsai-Wu Failure Criterion:

This failure theory is more general than the Tsai-Hill failure theory because it distinguishes between the compressive and tensile strength of

a lamina. The criteria is given by, [16].

$a\,\sigma_x^2 + b\,\sigma_x - 1 = 0$ .....(22)

where, $a = h_{11}\cos^4(\theta) + h_{22}\sin^4(\theta) + 2\,h_{12}\cos^2(\theta)\sin^2(\theta) + h_{66}\cos^2(\theta)\sin^2(\theta)$

$b = h_1\cos^2(\theta) + h_2\sin^2(\theta)$

and, $h_1 = \frac{1}{X_t} - \frac{1}{X_c}$, $h_{11} = \frac{1}{X_t X_c}$, $h_{22} = \frac{1}{Y_t.Y_c}$, $h_{66} = \frac{1}{S_t^2}$,

$$h_{12} = \frac{1}{2\sigma^2}\left[1 - (h_1 + h_2)\sigma - (h_{11} + h_{22})\sigma^2\right] .$$

(vi). Hashin-Rotem Criterion:

Two separate modes of failure mechanisms are proposed, one based on the failure of the fiber and the other based on the failure of the matrix. The first is governed by the longitudinal stress, with reference to the fiber orientation and the second is governed by the transversal and tangential stresses to the fiber. In this criterion, the failure modes of fiber failure and matrix failure are considered separately, [16].

$$\left(\frac{\sigma_{11}}{X_t}\right) \geq 1$$

Tensilefibre failure

$$\left(\frac{\sigma_{22}}{Y_t}\right)^2 + \left(\frac{\tau_{12}}{S_c}\right)^2 \geq 1$$

Tensile matrix failureTherefore, for an applied stress σ_x, the following equation applies for failure not occurs.

$$\min\left[\left(\left(\frac{Y_t}{\sin^2(\theta)}\right)^2 + \left(\frac{S_t}{\cos(\theta).\sin(\theta)}\right)^2\right), \left(\frac{X_t}{\cos^2(\theta)}\right)^2\right] \leq (\sigma_x)^2$$

.....(23)

(v). Hashin Failure Criteria

The main difference between this model and the previous Hashin and Rotem

model is that the fiber failure includes the contribution of □□$_{12}$) to the fiber failure in tension. Hence, for an applied stress (□$_x$) , the failure equations are, [17].

$$\left(\frac{\sin^2(\theta)}{Y_t}\right)^2+\left(\frac{\cos(\theta).\sin(\theta)}{S_t}\right)^2\le\left(\frac{1}{\sigma_x}\right)^2$$

…..(24)

$$\left(\frac{\cos^2(\theta)}{X_t}\right)^2+\left(\frac{\cos(\theta).\sin(\theta)}{S_t}\right)\le\left(\frac{1}{\sigma_x}\right)$$

…..(25)

The rmoelastic Properties

When the influence of temperature is taken into consideration, Hooke's law for the case of no temperature influence [12]:

$$\varepsilon=\frac{1+\nu}{\nu}\sum-\frac{\nu}{E}\mathrm{trace}(\sum)\mathbf{I};$$

is replaced by the *Hooke–Duhamel* law:

$$\varepsilon=\frac{1+\nu}{\nu}\sum-\frac{\nu}{E}\mathrm{trace}(\sum)\mathbf{I}+\alpha\Delta T\mathbf{I}$$

…….(26)

In the case of unidirectional composite the coefficient of thermal expansion of the matrix is usually much larger (more than ten times) than that of the fiber. One can imagine that even in the absence of mechanical loading, a change in temperature □*T* will produce a longitudinal strain in the composite. This longitudinal strain has a value that is intermediate between the strain of the fiber alone and that of the matrix alone. Then, in the composite one finds internal stresses along the direction *l* (along the direction *t*, the fiber and matrix can expand differently). One then has:

- For the stresses:

$$\sum_{matrix}=\begin{bmatrix}\sigma_l & 0\\ 0 & 0\end{bmatrix}_{matrix}$$

$$\sum_{fiber}=\begin{bmatrix}\sigma_l & 0\\ 0 & 0\end{bmatrix}_{fiber}$$

- For the strain:

$$\sum_{matrix}=\begin{bmatrix}\varepsilon_l & 0\\ 0 & \varepsilon_t\end{bmatrix}_{matrix}$$

$$\sum_{fiber}=\begin{bmatrix}\varepsilon_l & 0\\ 0 & \varepsilon_t\end{bmatrix}_{fiber}$$

Coefficient of Thermal Expansion along the Direction l:

One has for the fiber and the matrix, respectively [12]:

$$\varepsilon_l=\left\{\frac{\sigma_l}{E}\right\}_{matrix}+\alpha_{matrix}\Delta T=\varepsilon_l=\left\{\frac{\sigma_l}{E}\right\}_{fiber}+\alpha_{fiber}\Delta T$$

The external equilibrium can be written as:

$$(\sigma_l*e)_{matrix}+(\sigma_l*e)_{fiber}=0$$

where, taking into account the equality of the strains:

$$\left\{\frac{\sigma_l}{E}\right\}_m+\alpha_m\Delta T=-\sigma_{l_m}*\frac{e_m}{e_f}*\frac{1}{E_{fiber}}+\alpha_f\Delta T$$

$$\sigma_{l_m}=\frac{(\alpha_f-\alpha_m)\Delta T}{\frac{1}{E_m}+\frac{e_m}{e_f}*\frac{1}{E_f}}=\frac{(\alpha_f-\alpha_m)\Delta T}{\frac{1}{E_m}+\frac{V_m}{V_f}*\frac{1}{E_f}}$$

V represents the volume fraction. The longitudinal strain can then be written as:

$$\varepsilon_{l_m}=\varepsilon_{l_f}=\frac{(\alpha_f E_f V_f+\alpha_m E_m V_m)(\Delta T)}{E_f V_f+E_m V_m}$$

It is also the longitudinal strain that is created only by the effect of temperature:

$$\varepsilon_{l_m}+\varepsilon_{l_f}=\alpha_l\Delta T$$

where α_l is the longitudinal coefficient of thermal expansion. One can then equate the above expressions to obtain:

$$\alpha_l-\frac{(\alpha_f E_f V_f+\alpha_m E_m V_m)}{E_f V_f+E_m V_m}\qquad\ldots\ldots(27)$$

Coefficient of Thermal Expansion along the Transverse Direction (t):

The global thermal strain can be written as [12]:

$$\varepsilon_{t(global)} = \frac{\Delta(e_m + e_f)}{e_m + e_f} = \varepsilon_{t_m}\frac{e_m}{e_m + e_f} + \varepsilon_{t_f}\frac{e_f}{e_m + e_f}$$

Then:

$$\varepsilon_{t(global)} = \varepsilon_{t_m} * V_m + \varepsilon_{t_f} * V_f$$

Using the Hooke and Duhamel law [13]:

$$\varepsilon_{t(global)} = \left(-\sigma_{t_m} * \frac{V_m}{E_m} + \alpha_m \Delta T\right)V_m + \left(-\sigma_{t_f} * \frac{V_f}{E_{fiber}} + \alpha_f \Delta T\right)V_f$$

Using the expressions for stresses obtained before, one obtains:

$$\varepsilon_{t(global)} = \left\{\left(\alpha_m V_m + \alpha_f V_f\right) + \frac{\left(E_m V_f - E_f V_m\right)}{E_m V_m + E_f V_f} V_m V_f \left(\alpha_f - \alpha_m\right)\right\}\Delta T$$

The quantity between the brackets represents the coefficient of thermal expansion along the transverse direction *t*, α_t, which can be written as:

$$\alpha_{t(global)} = \left\{\left(\alpha_m V_m + \alpha_f V_f\right) + \frac{\left(E_m V_f - E_f V_m\right)}{\frac{E_m}{V_f} + \frac{E_f}{V_m}} \times \left(\alpha_f - \alpha_m\right)\right\} \quad \ldots(28)$$

Thermo-mechanical Behavior of a Unidirectional Layer:

Under the combined effect of the stresses and temperature, the global thermo-mechanical strains of a unidirectional layer can be obtained using the following relation:

$$\begin{Bmatrix} \varepsilon_1 \\ \varepsilon_2 \\ \gamma_{12} \end{Bmatrix} = \begin{bmatrix} \frac{1}{E_1} & \frac{\upsilon_{12}}{E_1} & 0 \\ \frac{\upsilon_{21}}{E_1} & \frac{1}{E_2} & 0 \\ 0 & 0 & \frac{1}{G_{12}} \end{bmatrix} \begin{Bmatrix} \sigma_1 \\ \sigma_2 \\ 0 \end{Bmatrix} + \Delta T \begin{Bmatrix} \alpha_1 \\ \alpha_2 \\ 0 \end{Bmatrix} \quad \ldots\ldots(29)$$

Results and Discussions

The results of this paper are illustrated below, from Figure (3) it can be seen that for unidirectional specimens, $[30]_4$, $[45]_4$, $[60]_4$ and $[90]_4$ the fracture has occurred in the direction of the fibres, this is an indication that the matrix has failed first. For the $[0]_4$ the fibre break has propagated through the matrix and to adjacent fibres. Figure (4) shows the failure mechanisms in cross-ply and angle-ply laminates are rather different to that observed in the unidirectional laminates. The failure usually starts at the weakest ply and the remaining plies may continue to support some load (not necessarily higher than the initial failure) until they reach their final strength limit.

Figure (5) shows the longitudinal elastic modulus E_1 for the unidirectional composite ($0°$ cut) is calculated for the fiber volume fraction range (*0 to 1*), all the considered models give near identical values for E_1 as a function of fiber volume fraction. Also shows the results of E_1 obtained from all the four models. The volume fraction which gave the best fit to the experimental results of E_1 corresponds to $V_f = 0.37$, a summary of the results at $V_f = 0.37$ are given in Table (2) for both $E_1$and E_2. Table (2) shows that the Halpin-Tsai model predicts the largest (E_2) value, while the strength of materials model (*SRoM*) gives the lowest value. The model that gives best fit to the measured values is that of Tsai with contiguity factor $C = 0$ and the *SRoM* model. The average value of the measured specimens $E_2 = 3.83$ *GPa* is verified by these models and is chosen to use in the theoretical calculations of the glass polystyrene composite at *0.37*-volume fraction.

Figure (6) shows the predicted values of Poisson's ratio (υ_{12}) from all four models as a function of fiber volume fraction (V_f), it was concluded that Tsai Model at contiguity factor $C=0$ gave the best fit to E_1 and E_2. Therefore, it is reasonable to assume that υ_{12} value equal 0.36 is a good estimate of the major Poisson's ratio of the unidirectional composite lamina using the expression given by this model. Figure (7) shows a graphical presentation of shear modulus (G_{12}) value as a function of volume

fraction, calculated from the expressions given by the four models. Experimentally, shear modulus (G_{12}) was calculated by using the results from off-axis tensile tests of unidirectional laminas at 30^o, 45^o, and 60^o using the expression derived from the relationship between the compliance matrix and stiffness matrix of angle lamina. From Figure (8), it can be seen that a sharp drop in stiffness occurs between 0^o to 30^o, after which there is no significant changes in stiffness with the off-axis load angle. A misalignment of 1 degree in the angle range 5^o to 20^o can result in stiffness change of up to 15%. Figure (9) shows the analysis results of five failure theories, it can be seen that the measured values are in a good agreements with Tsai-Wu and Tsai-Hill models. However, although the Hashin model is showing a discontinuity at ply angles between 15^o and 30^o, it also gives a good agreement with the measurements. The deviations from the measured values are more pronounced in the case of Hashin-Rotem and the Maximum Strength models. Figure (10) shows the failure analysis of the cross-ply and angle-ply laminates was also evaluated by applying the model in the lamination theory. The evaluation is based on dividing the laminate into sublamina and then calculating the strength factor for each layer by applying Tsai-Hill failure criteria. Figure (11) and (12) investigate the relation between the thermal expansion coefficient in the longitudinal $(\alpha_l)$and the transverse (α_t) directions for unidirectional and cross-ply specimens,$[0]_4$, $[30]_4$, $[45]_4$, $[60]_4$, $[90]_4$, [-45/45], [-15/75] and [0/90] out of the effects of measured values that essential to evaluate (α_l) and (α_t) to be based on the equations (27) and (28).

Conclusions:

From the results of this work the following conclusions can be obtained:

1-When applied load in the x-direction, the unidirectional lamina exhibits the highest strength. Among the layered laminates, the cross-ply laminate $[0/90]_s$ exhibits the highest strength compared to the angle ply laminates. This could be due to a none-dominating shear failure. Also, very little variations were observed in the strength between $[-15/75]_s$ and $[\pm 45]_s$ laminates.

2- The experimental results were in a good agreement with the lamination theory.

3- Tsai-Hill Failure criterion was found to fit best to the experimental data.

4- A good agreement between measurements and calculated strength was evident.

5- The strength analysis also showed that composite strength is strongly dependant on the fibre orientation, and it follows a similar trend to that of stiffness.

6- The failures of the specimens generally occurred in the form of fractures, macro-cracks or complete splitting into two parts, depending on the orientations of the fiber relative to the direction of applied load.

7- By comparing the experimental data with the predicted values of G_{12}, it was concluded that Tsai elasticity model with contiguity $C=0$ fits best to measured value.

8- The orientation angles increases of laminates for artificial composite has distinct effects upon the thermal expansion

coefficients α_l and α_t. It is evident that the increasing of α_l to be companion of the increasing in the angles of ply orientation in return for α_t decreases with certain angles. For cross-ply angles laminates, the values of α_l and α_t are closed together for each types that referred to.

References

[1]. Kullör L.P. and Spriner G.S., "Mechanics of Composite Structures", Cambridge University Press–Stanford, 2003.

[2]. Obrien, T.K., et al. "Influence of Specimen Preparation and Specimen Size on Composite Transverse Tensile Strength and Scatter". NASA/TM-2001-211030, ARL-TR-2540, 2001.

[3]. Urban, J. "Crushing and Fracture of Lightweight Structures", PhD Thesis, Technical University of Denmark, Dept. Mech. Eng., Material Engineering, Maritime Engineering, 2003.

[4]. El-Hajjar, R. F. "Experimental Study and Analytical Modeling of Tran slayer Fracture in Pultruded FRP Composites", PhD Thesis, Georgia Institute of Technology, school of civil and environmental engineering, 2004.

[5]. Perhi, P. K., Bhattacharyya, S. K. and Sinha, P. K. "Failure Analysis of Multiple Delaminated Composite Plates due to Bending and Impact", Indian Academy of Sciences, Materials Science Journal, Vol.24, No.2, pp. 143-149, 2001.

[6]. Tsai, S. W. and Wu, E. M. "A General Theory of Strength for Anisotropic Materials", J. Composite Materials, Vol.5, pp.58-80, 1971.

[7]. Paris, F. "A Study of Failure Criteria of Fibrous Composite Materials", NASA Report CR-210661, 2001.

[8]. A. Cherkaev, V. Vinogradov, "Bounds for Expantion Coefficients of Composites", *Department of Mathematics, University of Utah, 155 S 1400 E Salt Lake City Utah, 84112, USA*, 2004.

[9]. O. Sigmunda and S. Torquato,"Composites with extremal thermal expansion coefficients", Princeton University, Princeton, New Jersey, 1996.

[10]. ASTM D5687/D5687M-95 (2007). Standard Guide for Preparation of Flat Composite Panels with Processing Guidelines for Specimen Preparation. Book of Standards Volume: 15.03.

[11]. Hayder M. Al-Shukri, "Experimental and Theoretical Investigation into Some Mechanical Properties of Glass Polyester Composite under Static and Dynamic Loads", MSc Thesis, Engineering Electro-mechanics Department, University of Technology, 2007.

[12]. Daniel G. etal. "Composite Materials Design and Applications", CRC press LLC, USA, 2003.

[13]. ASTM D 3039/D 3039M (2005). Standard Test Methods for Tensile Properties of Polymer Matrix Composite Materials.

[14]. Department of Defense, "Composite Materials Handbook", Polymer Matrix Composites Materials Usage, Design and Analysis. MIL-

HDBK-17-3F Vol.3, USA, 2002

[15]. Icardi, U., Locatto, S. and Longo, A. "Assessment of Recent Theories for Predicting Failure of Composite Laminates", Applied Mechanics Reviews, Vol.60, pp.76-86, 2007.

[16]. Kuraishi, A.S. Tsai S.W. and Wang, J. "Material Charecterisation of Glass, carbon and Hybrid-Fiber SCRIMP panels", Contractor Report for Sandia National Laboratories, Contract 22163/SAND02-3538, 2002. http://www.osti.gov/bridge/servlets/purl/8085919JiZcu/native/808591.pdf

[17]. Mohsin, N. A., "Development of Composite Materials and Their Mechanical failure Characteristics", PhD Thesis, Dept. of Mechanics, University of Technology, Baghdad, 2003.

Table (1) The Apparent Elastic Modulus of Unidirectional Laminates with applied load in longitudinal direction

laminate	$[0_4]$	$[30_4]$	$[45_4]$	$[60_4]$	$[90_4]$	$[\pm 45]_s$	$[-15/75]_s$	$[0/90]_s$
$E_{apparent}$ (*GPa*)	19.84	6.94	5.15	4.01	3.83	5.55	9.17	11.97

Table (2) Theoretical and Experimental Results of E_1 and E_2 of Unidirectional Lamina at $V_f = 0.37$.

Model	E_1 *GPa*	E_2 *GPa*
SRoM	19.84	3.98
Halpin-Tsai	19.84	5.63
CCA	19.84	4.99
Tsai Elasticity C=0 C=0.1 C=0.2	19.84	 4.78 5.39 5.52
Measured Average	19.84	4.25

Table (3) Properties of Constituents [10]

Material	E (GPa)	*v*	G (GPa)	α (/K)
E-Glass fiber	$E_1 = 233$ $E_2 = 23.1$ $E_3 = 23.1$	$v_{12} = 233$ $v_{13} = 23.1$ $v_{23} = 23.1$	$G_{12} = 8.96$ $G_{13} = 8.96$ $G_{23} = 8.27$	$\alpha_1 = -0.54E-06$ $\alpha_2 = 10.1E-06$
Epoxy matrix	4.62	0.36	---	41.4E-06

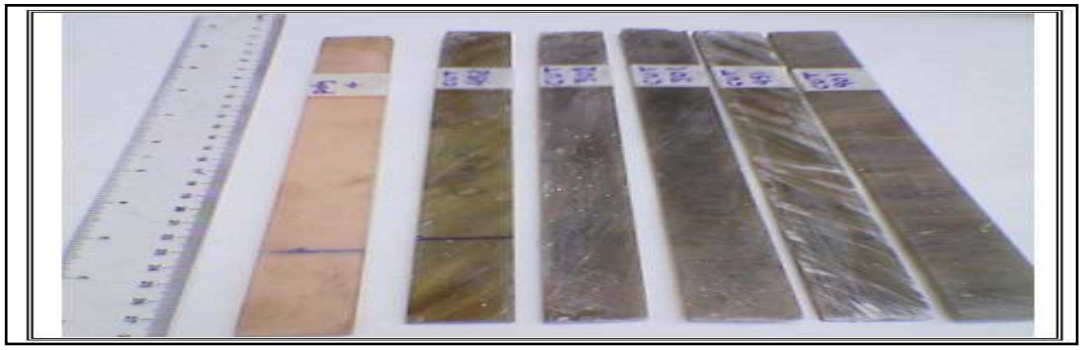

Figure (1) Unidirectional and Angle-ply Specimens

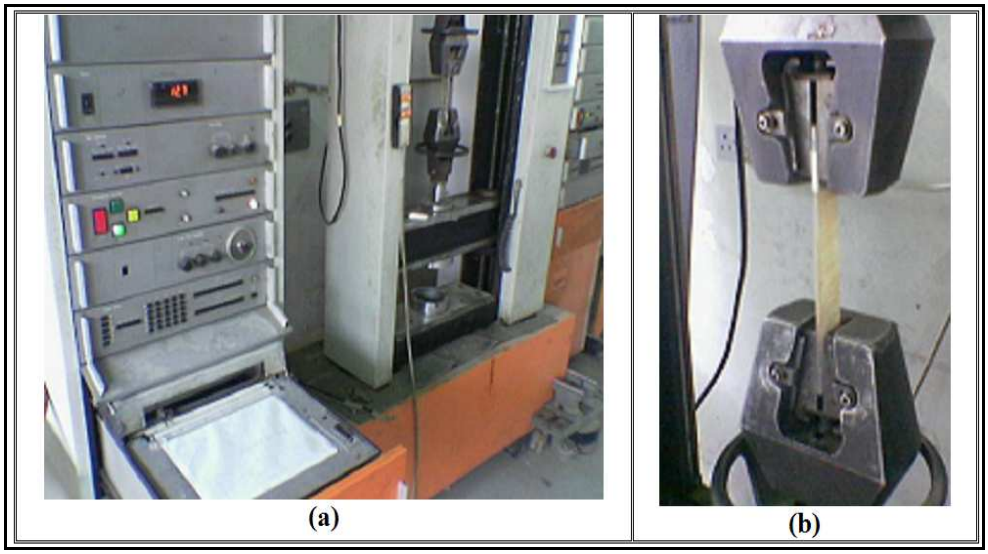

(a) **(b)**

Figure (2) (a) Instron 1195 Hydraulic Test Machine (b) Close up of Specimen Fixture

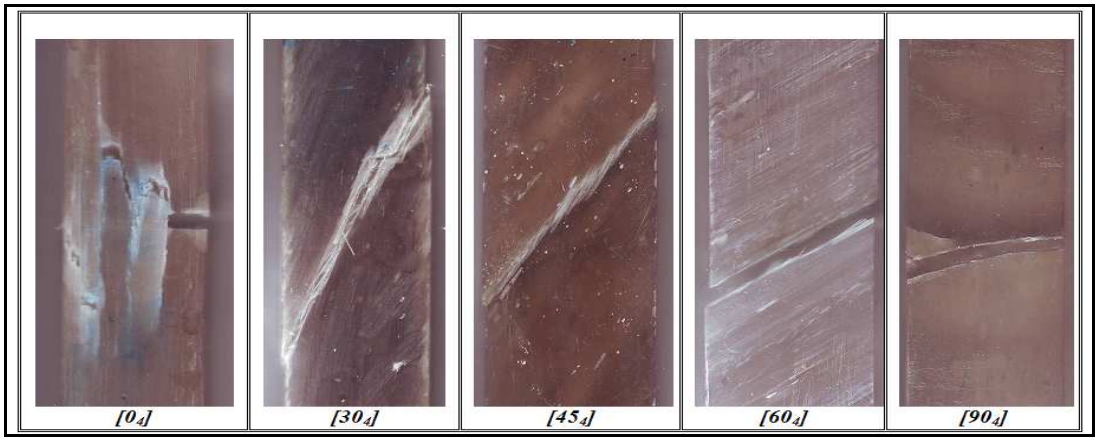

Figure (3) Unidirectional Specimens Fracture by Tensile Tests

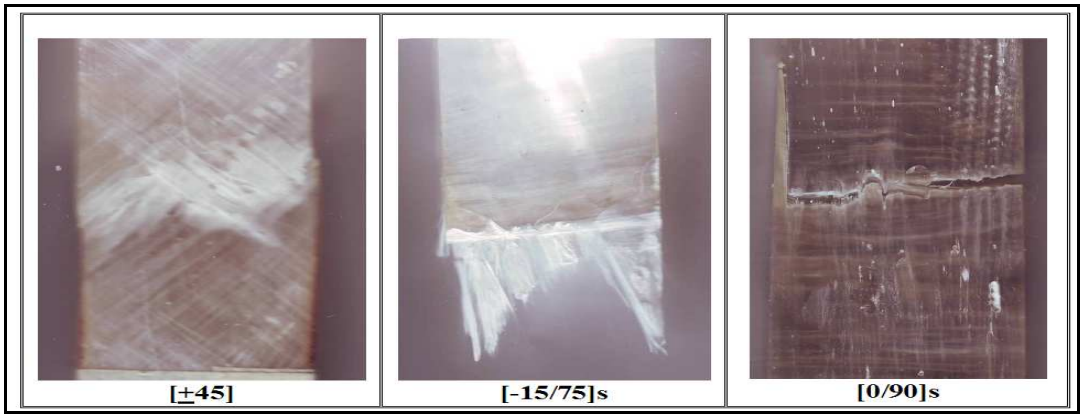

Figure (4) Angle-Ply Laminates Specimens after Tensile Tests

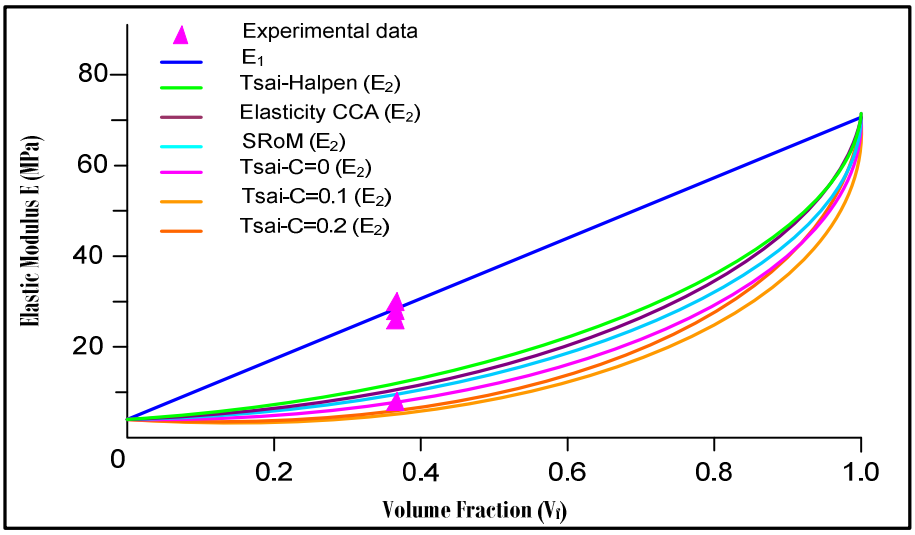

Figure (5) Experimental results and Models Prediction Of E_1 and E_2 of Unidirectional Lamina

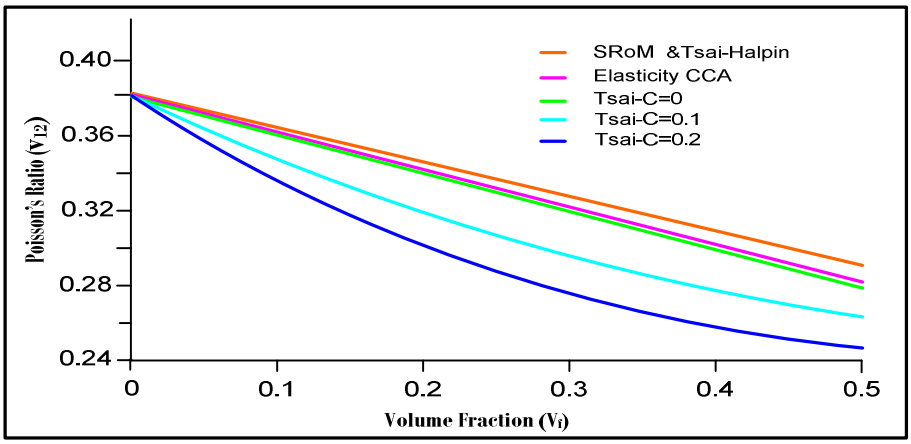

Figure (6) Models Prediction of Poisson's ratio (v_{12}) of Unidirectional Lamina

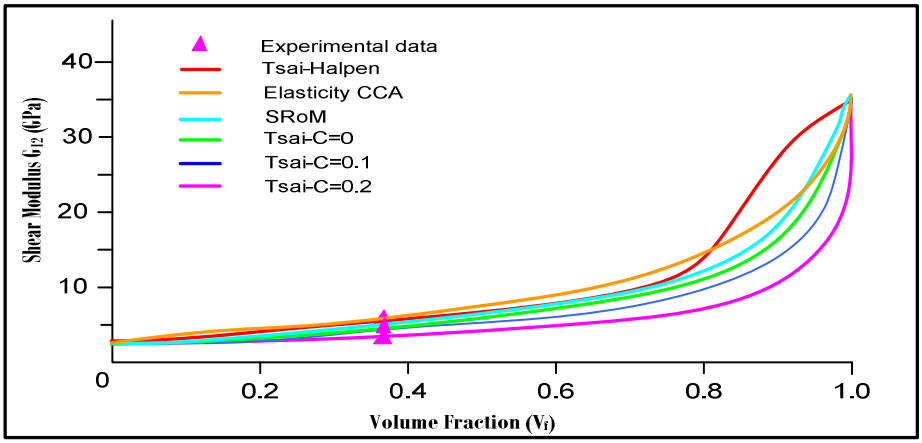

Figure (7) The Variation of Shear Modulus (G_{12}) with Volume Fraction (V_f)

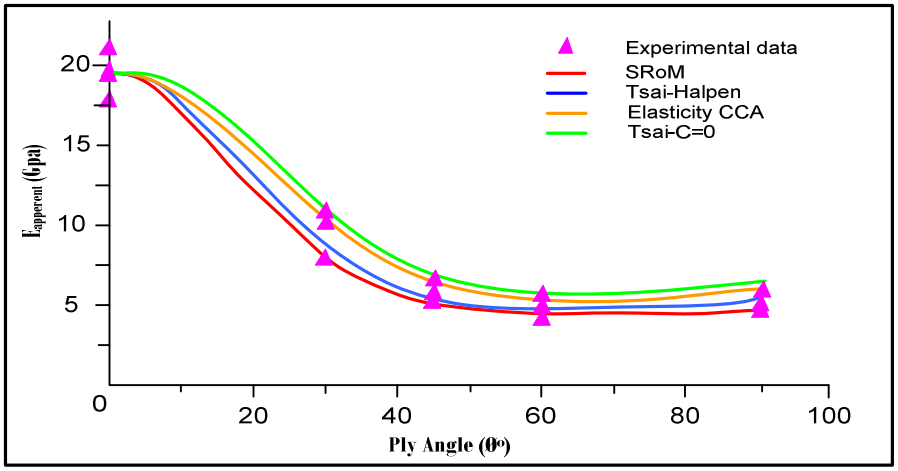

Figure (8) The Variation of Apparent Young's Modulus (E_x) with Angle-Ply Laminates

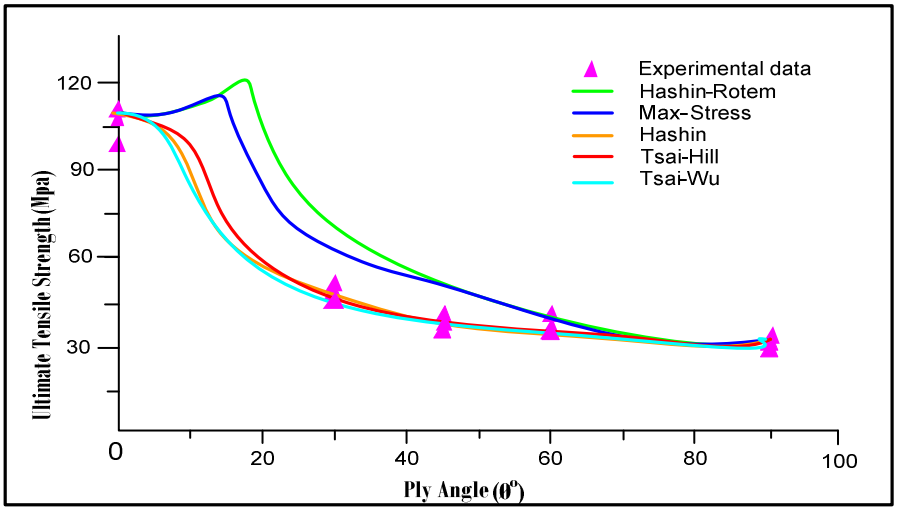

Figure (9)The Comparison Results of Failure Theories with Experimental results

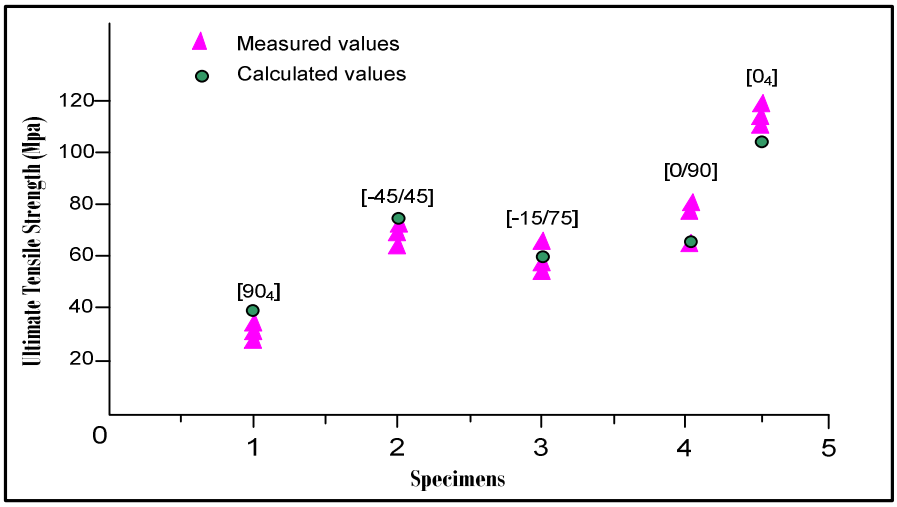

Figure (10) Strength of Glass - Polyester Composite Laminates

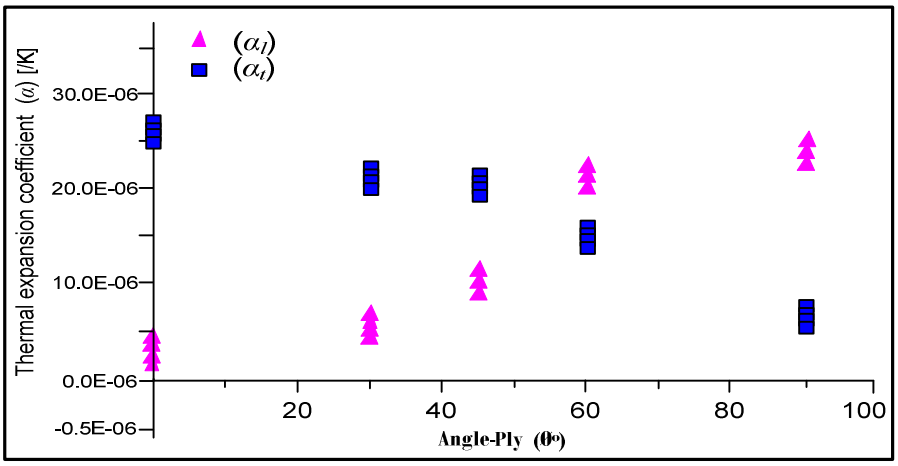

Figure (11) The Variation of Thermal expansion coefficient (α_l) and (α_t) with Unidirectional laminates

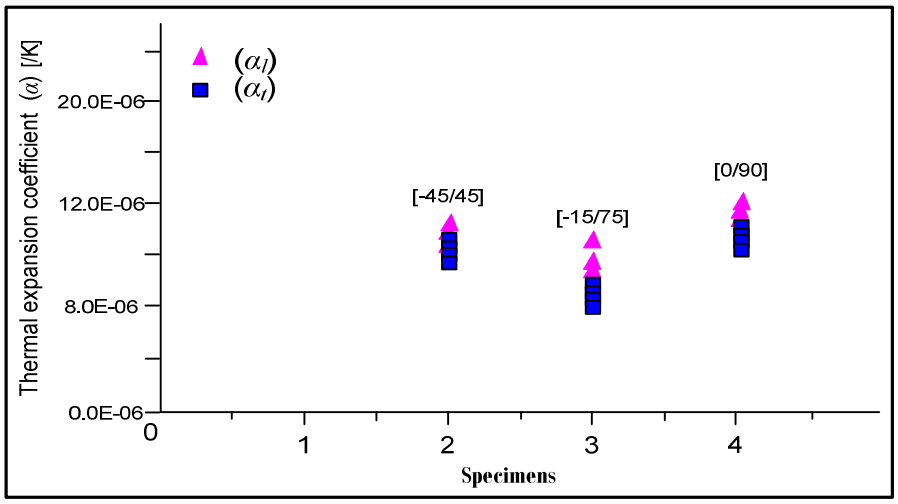

Figure (12) The Variation of Thermal expansion coefficient (α_l) and (α_t) with Cross-Ply Laminates